ARMY RESEARCH LABORATORY

Measured Infrared Absorption and Extinction Cross Sections for a Variety of Chemically and Biologically Derived Aerosol Simulants

by Kristan P. Gurton, Rachid Dahmani,
David Ligon, and Burt Bronk

ARL-TR-3253 June 2004

NOTICES

Disclaimers

The findings in this report are not to be construed as an official Department of the Army position unless so designated by other authorized documents.

Citation of manufacturer's or trade names does not constitute an official endorsement or approval of the use thereof.

Destroy this report when it is no longer needed. Do not return it to the originator.

Army Research Laboratory
Adelphi, MD 20783-1197

ARL-TR-3253 **June 2004**

Measured Infrared Absorption and Extinction Cross Sections for a Variety of Chemically and Biologically Derived Aerosol Simulants

Kristan P. Gurton, Rachid Dahmani, David Ligon
Computational and Information Sciences Directorate, ARL

Burt Bronk
Air Force Research Laboratory at ABCCOM

REPORT DOCUMENTATION PAGE

Form Approved
OMB No. 0704-0188

1. REPORT DATE *(DD-MM-YYYY)*	2. REPORT TYPE	3. DATES COVERED (From - To)
June 2004	Final	September 2003 to January 2004

4. TITLE AND SUBTITLE
Measured Infrared Absorption and Extinction Cross Sections for a Variety of Chemically and Biologically Derived Aerosol Simulants

5a. CONTRACT NUMBER

5b. GRANT NUMBER

5c. PROGRAM ELEMENT NUMBER

6. AUTHOR(S)
Kristan P. Gurton, Rachid Dahmani, David Ligon, and Burt Bronk

5d. PROJECT NUMBER
3FEJ00

5e. TASK NUMBER

5f. WORK UNIT NUMBER

7. PERFORMING ORGANIZATION NAME(S) AND ADDRESS(ES)
U.S. Army Research Laboratory
ATTN: AMSRD-ARL-CI-EE
2800 Powder Mill Road
Adelphi, MD 20783-1197

8. PERFORMING ORGANIZATION REPORT NUMBER
ARL-TR-3253

9. SPONSORING/MONITORING AGENCY NAME(S) AND ADDRESS(ES)
U.S. Army Research Laboratory
2800 Powder Mill Road
Adelphi, MD 20783-1197

10. SPONSOR/MONITOR'S ACRONYM(S)

11. SPONSOR/MONITOR'S REPORT NUMBER(S)

12. DISTRIBUTION/AVAILABILITY STATEMENT
Approved for public release, distribution unlimited.

13. SUPPLEMENTARY NOTES

14. ABSTRACT

In an effort to establish a more reliable set of optical cross sections for a variety of chemical and biological aerosol simulants, we have developed a flow-through photo-acoustic system capable of measuring the absolute, mass-normalized, extinction and absorption cross sections. By employing a flow-through design, we avoid issues associated with closed aerosol photo-acoustic systems and improve sensitivity. Although the results shown here were conducted over the tunable carbon dioxide laser waveband region (i.e., 9.20 to 10.80 μm), application to other wavelengths is easily achievable. Aerosols considered are categorized as biological, chemical, and inorganic in origin, i.e., bacillus subtilis endospores, dimethicone silicone oil (SF-96 grade 50), and Kaolin clay powder (alumina and silicate), respectively. Results compare well with previously measured spectral extinction using Fourier transform infrared spectroscopy. Comparison with Mie theory calculations based on previously published complex indices of refraction and measured size distributions is also presented.

15. SUBJECT TERMS
Aerosol, photo-acoustic, absorption, infrared, extinction

16. SECURITY CLASSIFICATION OF:			17. LIMITATION OF ABSTRACT	18. NUMBER OF PAGES	19a. NAME OF RESPONSIBLE PERSON
a. REPORT	b. ABSTRACT	c. THIS PAGE			Kristan P. Gurton
Unclassified	Unclassified	Unclassified	Ul	23	19b. TELEPHONE NUMBER (*Include area code*) (301) 394-2093

Standard Form 298 (Rev. 8/98)
Prescribed by ANSI Std. Z39.18

Contents

List of Figures

Acknowledgment

We would like to thank Dr. Paul Pellegrino and Dr. Nicholas Fell of the U.S. Army Research Laboratory for their continued supportand technical expertice.

INTENTIONALLY LEFT BLANK.

1. Introduction

Currently, there is great interest in developing both point and stand-off detection instrumentation capable of identifying the presence of harmful chemical and/or biological aerosols. Presently, the majority of sensors deployed in the field represent point detection schemes that are often based on a form of antibody tagging and/or chemical analysis that is conducted on collected samples. As a result, these methods often require periods on the order of several minutes for the chemical reaction to occur. Such time periods may prove critical in actual operation.

A more desirable approach would be a detection method based on *optical* interactions with the agent. Such an approach would allow for real-time detection/identification. In addition, by considering various tunable laser systems, one can envision a detection scheme based on a light detection and ranging (LIDAR) approach in which the detection of a chemical or biological release can be accomplished at great distances.

In order to design such systems, scientists and engineers will require a reliable, well-characterized database of optical constants for a variety of chemically and biologically derived aerosols, e.g., extinction, absorption, and scattering cross sections. Attempts to calculate these parameters have proved problematic for several reasons.

First, predictive calculations require that the real and imaginary indices of refraction for the aerosol be known with reasonable certainty. Unfortunately, such constants are woefully lacking. This is particularly true for biologically derived materials. When they do exist, issues of accuracy and applicability often arise (*1*).

Second, calculations for a polydispersed aerosol usually assume a certain particle size distribution when one is computing optical cross sections. Minor variation in either the breadth or form of these distributions can result in great uncertainty in the calculated cross sections.

Third, many of the computational techniques used to predict the electromagnetic interaction with small particles assume that the aerosol is of a particular simple shape, e.g., a perfect sphere. For most biologically derived agents, this is rarely the case. For example, assuming a complex particle to be an effective sphere becomes less valid as the dimensions of the particle approach the optical wavelength (*2*). Since many airborne bio-particles have sizes in the 0.8- to 12-μm range, optical techniques that rely on IR wavelengths operate where effective sphere calculations are prone to error (*3*).

As a result, we present a flow-through photo-acoustic technique (first proposed by Bruce et al.), which is designed to directly measure *in situ* the absolute mass normalized extinction, absorption, and total scatter cross sections for a variety of chemical, biological, and background aerosols (*4*,*5*,*6*). Previous attempts to apply photo-acoustic spectroscopy to aerosols used a

closed sample volume and as a result, were subject to nonuniform aerosol concentrations because of particle settling (*7*). In addition, such techniques were limited in sensitivity because of residual absorption of the transmission windows that resulted in signals that were comparable or greater than the absorption of the aerosol in question. In order to avoid these problems, Bruce designed an acoustically isolated flow-through cell that allowed for *in situ* analysis of moderate and weakly absorbing aerosols. With this design, high system sensitivities on the order of 0.001 km^{-1} are routinely achieved.

The materials considered for this study include dimethicone silicone oil (SF-96 grade 50), bacillus subtilis endospores (BG), and Kaolin clay, which represent chemical, biological, and natural background aerosols, respectively. For comparison, we present Mie theory calculation based on measured size distributions and previously published complex indices of refraction.

2. Experiment

Consider a sample volume containing an optically absorbing aerosol. If a laser is passed through this volume, a portion of the light will be absorbed by the aerosol particles, resulting in particle heating (here we assume that the absorption attributable the surrounding gas is negligible compared to the resultant particle absorption). This particle heating will subsequently result in a pressure rise within the sample volume. If the laser is now modulated at some convenient acoustic frequency, say 1 kHz, a resultant pressure wave will result at that same 1-kHz modulation frequency. It is well established that the power of the resultant acoustic signal is directly proportional to the optical absorption cross section of the absorbing particles (*8*). The constant of proportionality that relates the actual absorption cross section to the acoustic signal is determined via an appropriate calibration gas. One of the more intriguing aspects of aerosol photo-acoustics is that, in principle, it only depends on the fraction of light absorbed by the media and thus requires no *a priori* knowledge of aerosol particle shape, size, or complex refractive index. By designing a system in which the probe laser also serves as a coincident short-pass transmissometer, we can obtain an independent determination of the optical extinction simultaneously with the absorption measurement. As a result, accurate values of the single-scatter albedo are also determined when we find the difference between the total extinction and absorption.

The basic flow-through photo-acoustic measurement is shown in figure 1. As seen in the figure, the system consists of a small 0.6-m^3 aerosol chamber which is used to confine the dispersed aerosol. The chamber is flushed with dry air before each run in order to minimize any residual absorption attributable to water vapor. A small fan placed in the corner of the chamber is used to gently stir the aerosol to ensure that a uniform particle concentration is maintained.

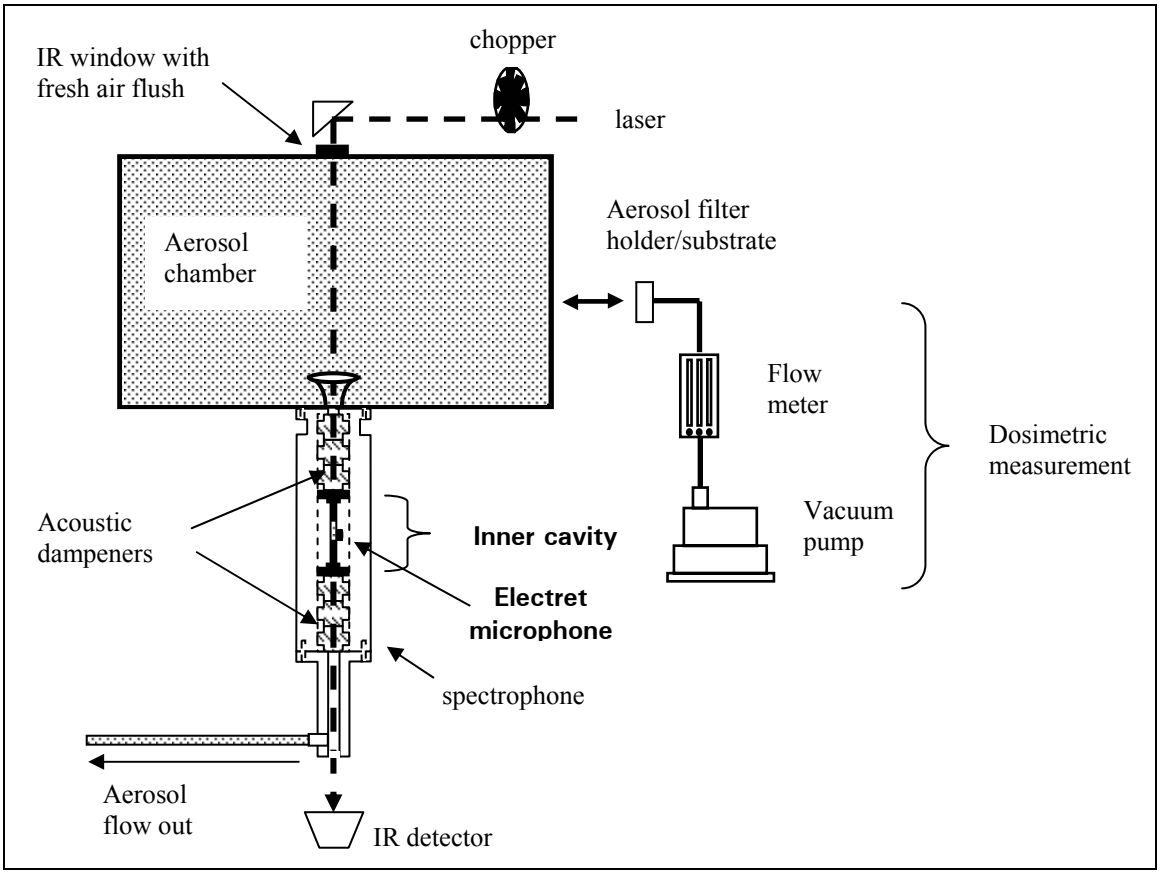

Figure 1. Schematic of flow-through photo-acoustic experiment used to measure *in situ* extinction and absorption cross sections.

Situated at the bottom of the chamber is a cylindrical flow-through spectrophone where both the extinction and absorption measurements take place. Embedded in the wall of the spectrophone is a highly sensitive electret microphone that is positioned in the center of a hollow cylindrical column in which the aerosol flows. A small (6 mm in diameter) electret condenser microphone consists of a high voltage internal membrane, a metal electrode, and a field effect transistor (FET). The microphone is externally powered through a simple RC circuit by a DC power supply. The diaphragm of the electret is mounted flush with the flow column in order to properly match the longitudinal acoustic mode generated within the cylindrical region. The inner cavity where the electret is mounted represents a resonant subsystem (basically, a double open-ended resonator) which is intentionally designed to be nonresonant, i.e., low Q values on the order of 20 to 50 for continuous wave (cw) sources, to avoid fluctuations in the spectrophone responsivity because of changing aerosol concentrations.

The dispersed aerosol is gently drawn from the chamber through the column that runs axially through the spectrophone. A modulated cw carbon dioxide (CO_2) laser, tuned to a specific IR wavelength and operated at approximately 100 mW, is directed through a barium fluoride (BaF_2) window, situated at the top of the chamber, and down through the center of the spectrophone.

The beam exits through a windowless port at the bottom of the spectrophone. We measure attenuation of the laser caused by the aerosol by placing an IR calorimetric power meter at the outlet of the spectrophone. This arrangement effectively creates a short-path transmissometer which extends from the top of the aerosol chamber to the bottom of the spectrophone. We established a well-defined aerosol path length caused by gently drawing the aerosol out of the spectrophone at a point just above the exit port. The path length used here was 1.22 m.

The modulated beam propagates through the center of spectrophone and a portion of its optical energy is absorbed by the aerosol. A rapid heating and subsequent cooling of the aerosol/air mixture occurs. This in turn produces an acoustic signal at the exact same frequency of the modulated laser beam. The acoustic wave signal is detected and amplified by the electret microphone via a "lock-in" amplifier tuned to the modulation frequency of the laser.

Shown in figure 1 is the aerosol dosimetry portion of the measurement which is used to determine the mass concentration at any point in time. We periodically take mass samples during the photo-acoustic measurement by drawing known volumes of the aerosol/air mixture through a filter substrate that is inserted into the chamber. The resultant mass is collected on pre-weighed polycarbonate filters, nominal pore size 0.20 μm, and is weighed with a high precision analytical balance. Resultant aerosol mass densities (g/m^3) are then used to convert path-integrated extinction/absorption coefficients (1/m) into mass normalized cross sections, (i.e., $meters^2/gram$).

Ambient acoustic noise resulting from movements within the laboratory is suppressed by a series of dampeners above and below the electret. The principle behind these acoustic dampeners is fairly straightforward (see figure 2). Shown in the figure is a cross-sectional schematic of a top set of three cylindrical dampeners. These dampeners fit snuggly together in the region surrounding the inner electret cavity and dissipate the acoustic noise that enters the spectrophone from either opening.

Both aerosol and acoustic "noise" from the laboratory flow freely through the center cylindrical region of the spectrophone. Acoustic noise enters the spectrophone in the form of pressure fluctuations that are initially distributed over the area of the inlet nozzle shown as point A in figure 2. For purposes of our example, let us define the area at point A to be 1.0 cm^2. As the pressure wave propagates down toward the inner electret cavity, it encounters several small spaces at point B in the figure. At these points, the pressure wave is effectively redistributed over a much larger area, say 30.0 cm^2, resulting in a reduction of the net pressure. The attenuation of the noise signal is repeated at each slit B until the desired noise suppression is achieved. We have found that a series of three or four dampeners placed above and below the electret cavity is sufficient to suppress typical noise levels encountered in the laboratory by approximately 20 dB at 1 kHz. Additionally, we isolate by machining the spectrophone enclosure from very dense materials, e.g., stainless steel or high density polyurethane.

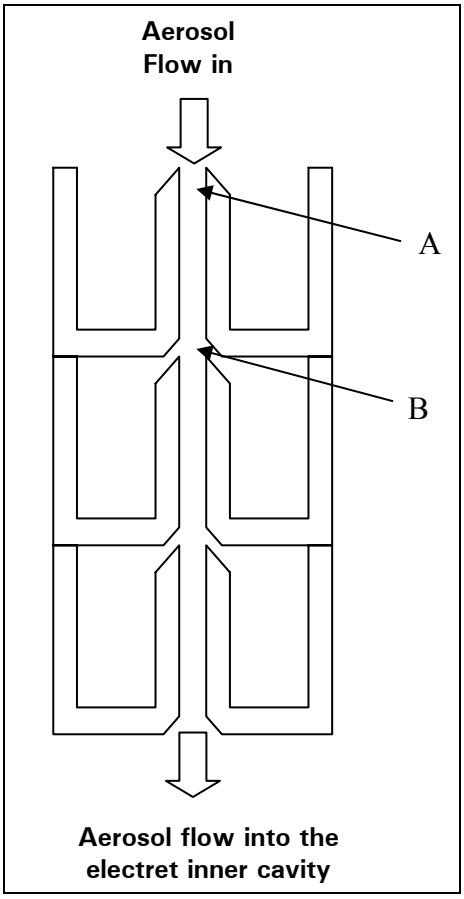

Figure 2. Cross-sectional schematic of a top set of acoustic dampeners used to isolate the electret inner cavity.

Simulants are dispersed in one of two ways. For small particulates such as powders, the aerosol is injected into the chamber via a dispersion nozzle and compressed dry air. The dispersion nozzle has a counter-rotating spiral array of stainless steel brushes that effectively separates the particles during dispersion.

If the simulant is a liquid, a pharmaceutical nebulizer is used. Approximately 20 psi of dry air are used to pump the nebulizer during dispersion, which produces a distribution, with a modal diameter in the 4- to 6-μm range.

Particle size distributions are measured *in situ* with an aerodynamic particle sizer (APS) (model 3321, manufactured by TSI, Inc.). Because the APS uses a "time-of-flight" method to predict an aerodynamic diameter, accurate values for the "bulk" density of the aerosol particle are required. Bulk densities used for BG, SF-96, and Kaolin were 1.45, 0.97, and 2.64 g/cm^3, respectively. The measured size distributions for the three simulants considered are shown in figure 3.

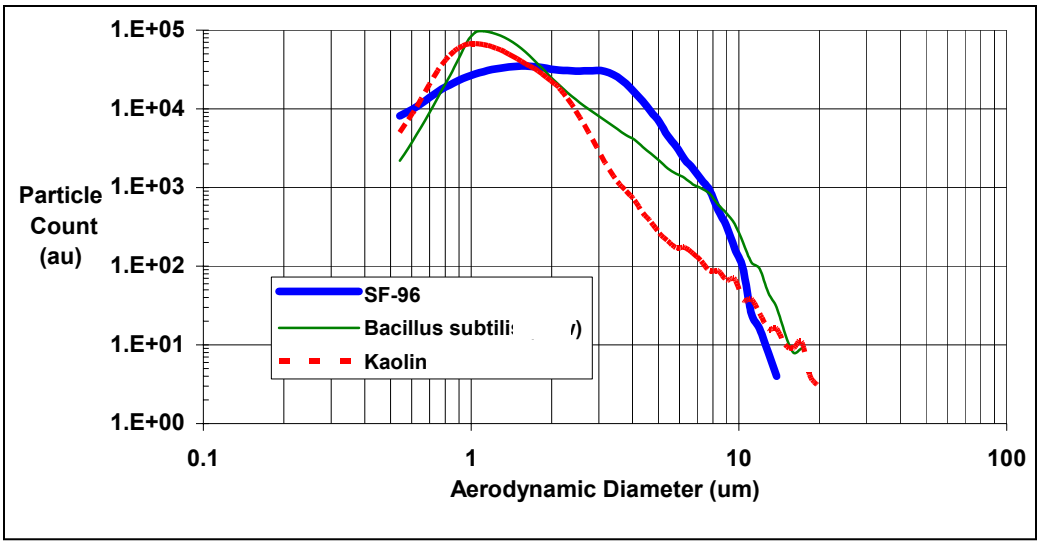

Figure 3. Measured size distributions for silicone oil SF-96, BG, and Kaolin clay aerosol.

We calibrate the system before and after each run by inserting an appropriate absorbing gas into the spectrophone cell. For CO_2 laser wavelengths, isopropyl alcohol or methanol vapor is used and provides adequate absorption *and* extinction of the IR laser over the tunable range of 9.2 to 10.8 μm. As the vapor is drawn through the system, a portion of the laser energy is absorbed, resulting in an acoustic signal that is detected by the spectrophone. This absorbed energy is seen as a reduction in the overall laser power as measured by the calorimetric meter and is converted to an absolute extinction coefficient via the Beer's law relation. Because the attenuating media is a gas, no scattering is present (we have assumed that attenuation by molecular scatting is negligible). In this situation, the path-integrated total extinction (1/m) of the CO_2 laser is *equal* to the measured absorption or, more precisely, to the acoustic response of the spectrophone. A typical calibration based on isopropanol vapor is shown in figure 4.

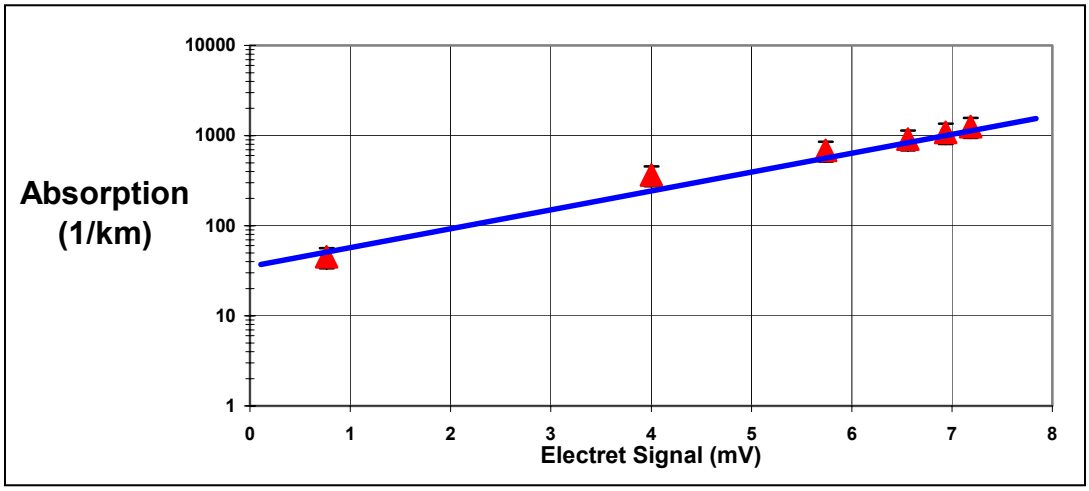

Figure 4. Typical calibration curve for the photo-acoustic spectrophone with isopropanol vapor.

3. Results

Figures 5 through 7 show the mass normalized extinction and absorption for aerosolized SF-96 oil, BG, and Kaolin clay, respectively.

Each of the three graphs shows a comparison between two separate and independent measurements, i.e., the spectral extinction measured with photo-acoustics or a previous *in situ* FTIR measurement conducted by the authors (*9*). Identical methods for dissemination were applied in both cases in an attempt to generate similar size distributions. In addition to the comparison between the two spectroscopic methods, measured cross sections are compared with a series of Mie theory calculations based on previously published complex indices of refraction and the actual size distributions shown in figure 3 (*10*,*11*,*12*).

Because great effort was taken to duplicate conditions between the photo-acoustic and FTIR studies, we would expect the spectral extinction to compare well between the photo-acoustic (red data points) and the FTIR results (red solid line). As one can see in figures 5 through 7, agreement between the two independent measurements appears quite good. However, comparison between the measured quantities and the Mie calculated values does not track quite as well. One possible reason for the apparent disagreement may lie in the choice of refractive indices used in our calculations.

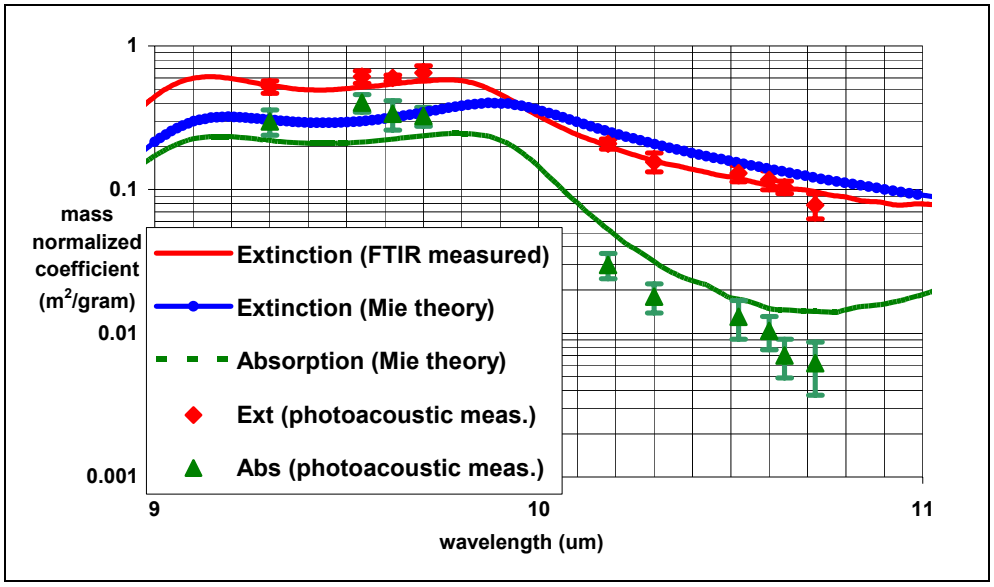

Figure 5. Comparison of the measured and calculated extinction and absorption cross sections for silicone oil SF-96, grade 50. (The individual data points seen in the figure represent the photo-acoustic measured cross sections. The solid [red] line represents previously measured spectral extinction with FTIR aerosol spectroscopy. The solid [blue] and dashed [green] lines represent Mie theory calculations based on the size distributions seen in figure 3 and the previously published complex indices of Querry (*12*).)

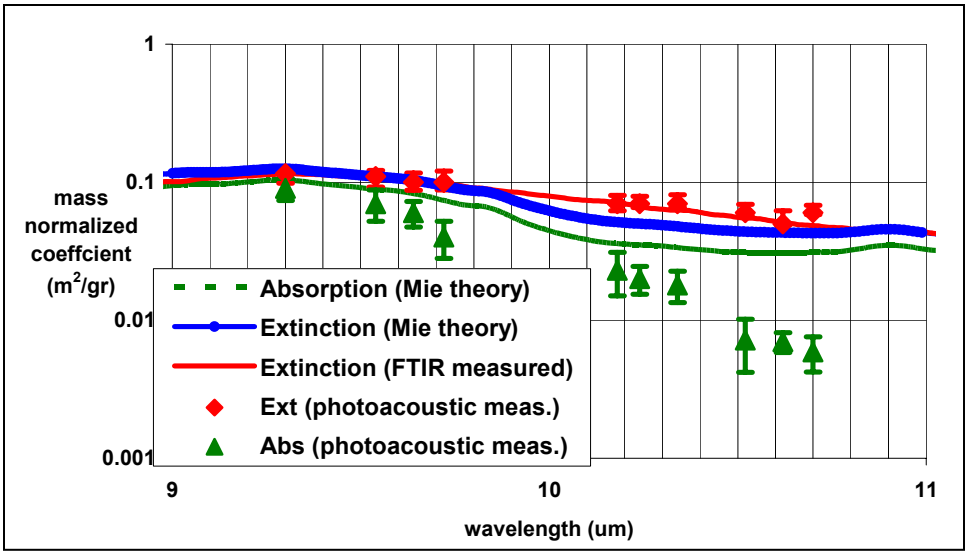

Figure 6. Comparison of the extinction and absorption cross sections for aerosolized BG endospores. (The individual points seen in the figure represent the photo-acoustic measured cross sections. The solid [red] line represents previously measured spectral extinction with FTIR aerosol spectroscopy. The remaining dashed [green] and solid [blue] lines represent Mie theory calculations based on the size distributions seen in figure 3 and the previously published complex indices of Querry (*12*).)

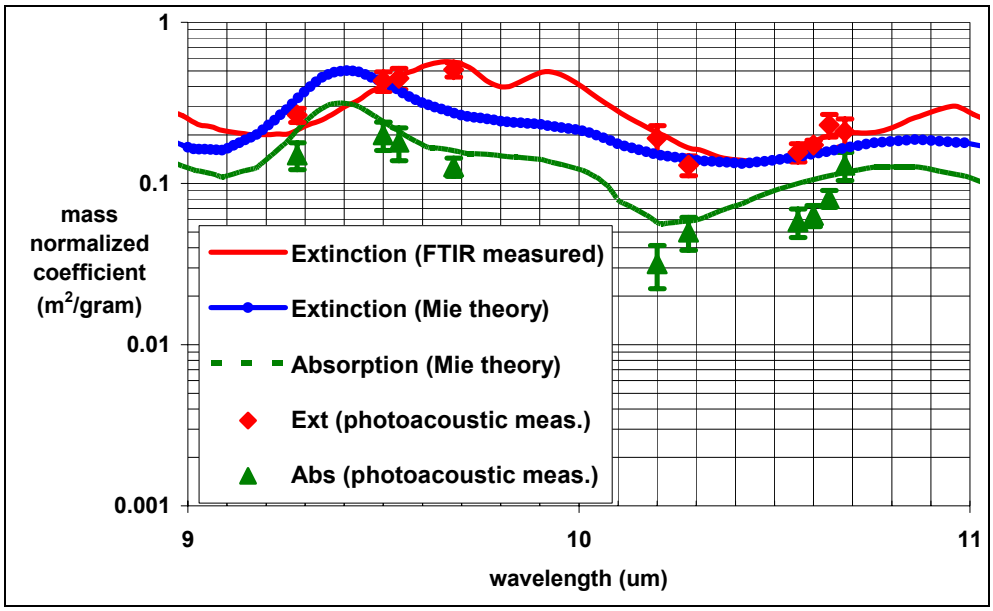

Figure 7. Comparison of the extinction and absorption cross sections for aerosolized Kaolin clay powder. (The individual points seen in the figure represent the photo-acoustic measured cross sections. The solid [red] line represents spectral extinction previously measured with FTIR aerosol spectroscopy. The remaining dashed [green] and solid [blue] lines are the corresponding Mie theory calculations based on the size distributions seen in figure 3 and the previously published complex indices of Querry (*12*).)

Often, researchers must rely on optical constants derived from much earlier work when they are calculating certain coefficients. In cases when there is a high degree of standardization for the material in question, the optical constants determined from a particular sample most probably represent the material as a whole, e.g., commercially manufactured chemicals or powders. However, for substances that are created by a natural process, samples of a particular material may vary greatly.

For example, the best overall agreement appears to be with the chemical simulant SF-96. The reason for this originates in the standard form in which the material is manufactured, i.e., produced by one vendor with a high degree of quality control. As a result, we believe the SF-96 indices measured by Querry are the most accurate of the three simulants considered.

In addition to issues of standardization between samples, great uncertainties can arise in reflective/transmissive techniques used to determine complex indices of refraction when conducted on powdered bulk materials, i.e., BG and Kaolin (*13*). Such methods are more accurate when conducted on liquids since they avoid problems with multiple scattering often seen in bulk sample "pellets". Figures 6 and 7 highlight the magnitude of the uncertainty one might expect when computing certain cross sections based on indices of refraction derived from previous studies.

Figure 6 shows the measured and calculated extinction and absorption for aerosolized BG endospores. Seen in the figure is the noticeable divergence that takes place between the measured absorption (green data points) and the calculated values based on Mie theory. We believe the primary reason for the disagreement stems from the fact that our endospore samples underwent a certain preparation in order to facilitate efficient dispersion and may not represent the spectroscopic grade bacillus subtilis used by Querry. Ion chromatography performed on both washed and unwashed endospore suspensions show small quantities of SO_4^{-2} with lesser amounts of PO_4^{-3}, F^-, and Cl^- ions, which have been attributed to small quantities of either a surfactant or residual growth media (*14*). Figure 7 shows a similar comparison for a Kaolin clay aerosol. Since Kaolin is mined throughout the globe and prepared by many different vendors, it was uncertain how "standard" our samples were. Again, we had to rely on previously measured indices of refraction. As one can see in figure 7, the agreement is reasonable, considering the number of unknown variables involved among the naturally occurring substances such as BG and/or Kaolin.

4. Conclusion

We have successfully developed an *in situ* flow-through photo-acoustic technique that is capable of directly measuring the absolute mass normalized extinction and absorption for a variety of biologically and chemically based aerosols. The flow-through design avoids problems that have plagued previous attempts at applying photo-acoustics to an aerosol medium. Although the results presented here were conducted at selected CO_2 laser wavelengths, any convenient laser source capable of tens of milliwatts of power would suffice. Photo-acoustic results compare well with prior FTIR measured spectral extinction.

Finally, for comparison we have provided several Mie theory calculations that used the best available values for the complex indices of refraction and measured size distributions. Comparison of measured and Mie theory computed cross sections highlights the typical uncertainties one might expect when conducting similar predictive calculations.

5. References

1. Wieliczka, D.; Querry, M. *Four Techniques to measure complex refractive indices of liquids and solids at carbon dioxide laser wavelengths in the infrared spectral region*; CRDEC-CR-062; U.S. Army Chemical Research, Development & Engineering Center, Jan. 1990.

2. Bohren, C.; Huffman, D. Absorption and Scattering of Light by Small Particles, *Wiley-Interscience Press* **1983**, New York, NY.

3. Wick, C.; Edmonds, R.; Blew, J. *Rapid detection and identification of background levels of airborne biological particles*; ERDEC-TR-155; Edgewood Research, Development & Engineering Center, Jan. 1995.

4. Bruce, C.W.; Pinnick, R.G. In-situ measurements of aerosol absorption with a resonate cw laser spectrophone. *Appl. Opt.* **1977**, *16* (7), 1762–1765.

5. Bruce, C.W.; Richardson, N.M. Propagation at 10 μm through smoke produced by atmospheric combustion of diesel fuel. *Appl. Opt.* **1983**, *22* (7), 1051–1056.

6. Bruce, C.W.; Stromberg, T.F.; Gurton, K.P. Trans-Spectral Absorption and Scattering of Electromagnetic Radiation by Diesel Soot. *Appl. Opt.* **1991**, *30* (12), 1537–1546.

7. Roessler, D.M.; Faxvog, F.R. Optoacoustic measurement of optical absorption in acetylene smoke. *J. Opt. Soc. Am.* **1979**, *69* (12), 1699–1704.

8. Rosencwag, A. Photoacoustics and Photoacoustic Spectroscopy, *Krieger Pub.*, New York (1990).

9. A detailed description of our FTIR measurements conducted on a variety of chemical and biological aerosols are at the time of this writing being considered for future publication in Appl. Opt.

10. Gurton, Kristan, P.; Ligon, D.; Kvavilashvili, R.; Kvavilashvili, Measured infrared spectral extinction for aerosolized Bacillus subtilis var. niger endospores from 3 to 13um. *Appl. Opt.* **2001**, *40* (25), 4443–4448.

11. Gurton, Kristan P.; Ligon, David; Dahmani, Rachid. *In situ measurement of the infrared spectral extinction for various chemical, biological, and background aerosols*; ARL-TR-3071; U.S. Army Research Laboratory: Adelphi, MD, Sept. 2003.

12. Querry, Marvin R. *Optical constants of minerals and other materials from the millimeter to the ultraviolet*; CRDEC-CR88009; Chemical Research, Development and Engineering Center, November 1987.

13. Wieliczka; Querry, M. *Four techniques to measure complex refractive indices of liquid and solids at carbon dioxide laser wavelengths in the infrared spectral region*; CRDEC-CR-062; Chemical Research, Development & Engineering Center, Jan. 1990.

14. Pellegrino, P.M.; Fell, N.F., Bacterial endospore detection using terbium dipicolinate photoluminescence in the presence of chemical and biological materials. *Anal. Chem.*, **1998**, *70*, 1755–1760.

Distribution

ADMNSTR
DEFNS TECHL INFO CTR
ATTN DTIC-OCP (ELECTRONIC COPY)
8725 JOHN J KINGMAN RD STE 0944
FT BELVOIR VA 22060-6218

DARPA
ATTN IXO S WELBY
3701 N FAIRFAX DR
ARLINGTON VA 22203-1714

OFC OF THE SECY OF DEFNS
ATTN ODDRE (R&AT)
THE PENTAGON
WASHINGTON DC 20301-3080

US ARMY TRADOC
BATTLE LAB INTEGRATION & TECHL DIRCTRT
ATTN ATCD-B
10 WHISTLER LANE
FT MONROE VA 23651-5850

DIR FOR MANPRINT OFC OF THE
DEPUTY CHIEF OF STAFF FOR PRSNNL
ATTN J HILLER
THE PENTAGON RM 2C733
WASHINGTON DC 20301-0300

EDGEWOOD CHEMICAL BIOLOGICAL CTR
ATTN AMSSB-RRT-DP A C SAMUELS
ATTN AMSSB-RRT-DP R VANDERBEEK
5183 BLACKHAWK RD BLDG E-5554
ABERDEEN PROVING GROUND MD 21010-5424

SMC/GPA
2420 VELA WAY STE 1866
EL SEGUNDO CA 90245-4659

US ARMY ARDEC
ATTN AMSTA-AR-TD
BLDG 1
PICATINNY ARSENAL NJ 07806-5000

US ARMY AVIATION & MIS LAB
ATTN AMSAM-RD-MG-IP H F ANDERSON
REDSTONE ARSENAL AL 35809

US ARMY AVN & MIS CMND
ATTN AMSMI-RD W C MCCORKLE
REDSTONE ARSENAL AL 35898-5240

US ARMY CECOM RDEC NVESD
ATTN J HOWE
10221 BURBECH RD STE 430
FT BELVOIR VA 22060-5806

US ARMY ECBC
ATTN AMSSB-RRT BOTTIGER
ATTN AMSSB-RRT E STUEBING
5183 BLACKHAWK RD BLDG E-5951
ABERDEEN PROVING GROUND MD 21010-5424

US ARMY INFO SYS ENGRG CMND
ATTN AMSEL-IE-TD F JENIA
FT HUACHUCA AZ 85613-5300

US ARMY NATICK RDEC
ACTING TECHL DIR
ATTN SBCN-TP P BRANDLER
KANSAS STREET BLDG78
NATICK MA 01760-5056

US ARMY SIMULATION TRAIN &
INSTRMNTN CMND
ATTN AMSTI-CG M MACEDONIA
12350 RESEARCH PARKWAY
ORLANDO FL 32826-3726

USAF ARMSTRONG LAB EDGEWOOD RDEC
ATTN AMSSB-RRT B BRONK
BLDG E-5951
ABERDEEN PROVING GROUND MD 21010

NAV RSRCH LAB
ATTN J D EVERSOLE
4555 OVERLOOK AVE
WASHINGTON DC 20375

HICKS & ASSOC INC
ATTN G SINGLEY III
1710 GOODRICH DR STE 1300
MCLEAN VA 22102

DIRECTOR
US ARMY RSRCH LAB
ATTN AMSRD-ARL-RO-D JCI CHANG
PO BOX 12211
RESEARCH TRIANGLE PARK NC 27709

US ARMY RSRCH LAB
ATTN AMSRD-ARL-CI-EE K GURTON
(10 COPIES)
ATTN AMSRD-ARL-CI-IS MAIL & RECORDS
MGMT
ATTN AMSRD-ARL-CI-OK-T TECHL PUB
(2 COPIES)
ATTN AMSRD-ARL-CI-OK-TL TECHL LIB
(2 COPIES)

US ARMY RSRCH LAB (cont'd)
ATTN AMSRD-ARL-D J M MILLER
ATTN AMSRD-ARL-SE-EE A GOLDBERG
ATTN AMSRD-ARL-SE-EM D BEEKMAN
ATTN AMSRL-SE-PO P PELLEGRINO
ADELPHI MD 20783-1197